

# Rapid onset of strain relief by massive generation of misfit dislocations in Bi(111)/Si(001) heteroepitaxy

Cite as: Appl. Phys. Lett. **114**, 081601 (2019); doi: [10.1063/1.5088760](https://doi.org/10.1063/1.5088760)

Submitted: 14 January 2019 · Accepted: 7 February 2019 ·

Published Online: 25 February 2019



View Online



Export Citation



CrossMark

D. Meyer, G. Jnawali,<sup>a)</sup>  H. Hattab, and M. Horn-von Hoegen<sup>b)</sup> 

## AFFILIATIONS

Department of Physics and Center for Nanointegration Duisburg-Essen (CENIDE), University of Duisburg-Essen, Lotharstr. 1, 47057 Duisburg, Germany

<sup>a)</sup>Present address: Department of Physics, University of Cincinnati, ML0011, 400 Geology/Physics Bldg., Cincinnati, OH 45221, USA

<sup>b)</sup>Author to whom correspondence should be addressed: [horn-von-hoegen@uni-due.de](mailto:horn-von-hoegen@uni-due.de)

## ABSTRACT

Strain and its relaxation in lattice mismatched heterostructures are crucial for the functionality of modern electronic devices, which are often challenging to determine experimentally. Here, we demonstrate a technique for measuring the strain state during epitaxial growth of Bi(111) films on Si(001) by using the spot profile analysis low-energy electron diffraction. Exploiting two non-equivalent integer-order diffraction spots originated from two Bi sub-lattices, the lattice parameter of the film is determined with high precision, which allows tracing the strain state as the film grows. The sudden and massive generation of misfit dislocations is found at a critical thickness of 4 nm which is explained through the inhomogeneous strain state of films with a thickness below one quarter of the mean distance of the dislocations.

Published under license by AIP Publishing. <https://doi.org/10.1063/1.5088760>

The strain state of lattice-mismatched systems is of crucial importance to the specific electronic functionality of heterostructure devices in the modern semiconductor industry. Even with subtle changes in the lattice parameter of a strained heterofilm, the band structure of the film is modified, which eventually affects the transport and optical properties of the heterostructure devices.<sup>1–3</sup> This interrelation between the strain state and the resulting modifications of the electronic structure of the heterosystem is employed as strain-state engineering to design high speed silicon devices<sup>4,5</sup> as well as for closing the “green gap” for efficient light emitting diodes by using strained III–V semiconductor devices.<sup>6–9</sup> With the occurrence of plastic relaxation through defects or misfit dislocations, however, the electronic transport properties of the devices are usually ruined. It is thus of fundamental importance to understand the kinetics of dislocation generation beyond a level of knowledge of a critical thickness  $d_c$  when the first misfit dislocation is generated. It is equally important to develop strategies to control the formation of dislocations in heteroepitaxial systems, which requires accurate and *in-situ* measurements of the strain state and the critical thickness of strain relaxation.

Experimental methods at present hardly allow a detailed real time and atomic level study of the interface of a heterosystem

during the formation of strain relieving misfit dislocations. Electron diffraction-based techniques were used to investigate the strain state in epitaxial systems due to their surface sensitivity.<sup>10,11</sup> Spot profile analysis low-energy electron diffraction (SPA-LEED) offers great advantages over other techniques due to its high dynamic range and possibility of real time measurements.<sup>12–14</sup> Therefore, we use SPA-LEED and its functional capabilities to precisely determine the strain state of anisotropically strained heteroepitaxial systems. We take advantage of the intrinsic property of heterosystems with anisotropic strain, which presuppose different crystallographic orientations for the substrate and the heterofilm, e.g., a (111) film on a (001) substrate. We introduce an approach of using the relative change of neighboring reflex positions as a highly sensitive magnifying glass for the determination of relative lattice parameters. Because this technique takes advantage of the relative position of two non-equivalent diffraction spots, it is robust against any non-linearity or distortion in the diffraction pattern. This method can be applied to a variety of diffraction techniques such as low-energy electron diffraction (LEED), reflection high-energy electron diffraction, transmission electron diffraction, or X-ray diffraction. Most importantly, from the practical viewpoint, this method is insensitive to thermal drift and thermal expansion of the

substrate or of the heterofilm and can be used at different temperatures, i.e., during annealing cycles of a heterofilm.

Here, we employ this method for probing the strain relaxation within the lattice mismatched Bi(111)/Si(001) heteroepitaxial system. We observe a rapid onset of strain relaxation during growth as the film thickness exceeds the critical thickness  $d_c = 4$  nm for strained growth of a coherent film on Si(001). Surprisingly, within an additional 3 nm growth of the Bi film beyond  $d_c$ , already 2/3 of the strain is relieved. The relaxation sets in with a massive generation of misfit dislocations at  $d_c$  which is followed by a regime of delayed and slow generation of misfit dislocations. Such a rapid onset of strain relaxation is explained by inhomogeneous strain relief due to the local confinement of strain fields in the heterofilm. The subsequent slow generation of dislocations is governed by existing theories assuming homogeneous strain relief.

The lattice structure of Bi(111) and its commensurability with Si(001) have been investigated previously.<sup>15–17</sup> Due to the fourfold symmetry of the substrate, the Bi(111) film grows with two domains rotated by 90°. The match of the two lattices is schematically shown in Fig. 1(a). Along the  $[1\bar{1}0]$  direction, 11 Bi atomic distances of 4.54 Å fit well on 13 Si atomic distances of 3.84 Å. Along the  $[\bar{1}10]$  direction, the Bi(111) film is relaxed. The corresponding separation of the diffraction spots is in accordance with Bi bulk values. Along the perpendicular  $[110]$  direction, a compression of the Bi film by 2.3% ( $\epsilon = -0.023$ ) is sufficient that both lattices are in registry: the Bi row distance of 3.93 Å fits except for a mismatch of only 2.3% to the Si row distance of 3.84 Å.

In this situation, the hexagonal diffraction pattern of the Bi(111) film is stretched by  $(1 + \epsilon)^{-1} \cong (1 - \epsilon) \cong 2.3\%$  along the  $[110]$  direction. Such an anisotropic distortion of the diffraction pattern is difficult to observe through an absolute determination of the spot position. The superposition of the two distorted diffraction patterns which are rotated by 90° renders the ingenious possibility to employ the relative separation between spots originating from the two hexagonal sublattices for the determination of the strain state.

In the left top panel of Fig. 1(b), the superposition of two undistorted Bi(111) diffraction patterns rotated by 90° is shown. Obviously, few of the fourth order integer order spots, namely, the  $(14)$  and  $(41)^*$  spots (15°-spots) and the  $(43)^*$  and  $(13)$  spots (45°-spots) from the two sub-patterns, are very close. During changes in the strain state, the relative separation of these pairs of spots changes notably when—as shown in the lower left panel of Fig. 1(b)—the Bi(111) film is commensurate with the Si substrate in the  $[110]$  direction, i.e., compressed by 2.3%, i.e.,  $\epsilon_{110} = -0.023$ . While the change of the absolute positions is hard to identify, the relative change of the separation and the position of the 15° and 45° spots is easily seen. The variation of the spot position for different anisotropic strain states  $\epsilon$  is plotted in the right panels of Fig. 1(b). The distance  $\Delta_{45^\circ}$  of the two 45° spots is given by

$$\Delta_{45^\circ} = \frac{2\pi}{a_0} \sqrt{2} \left( 3 \frac{\sqrt{3}}{2} - \frac{5}{2} + \frac{5}{2} \epsilon_{110} \right).$$

The distance  $\Delta_{45^\circ}$  between the 4th order spots of the two sub-patterns is more than doubled during relaxation of the

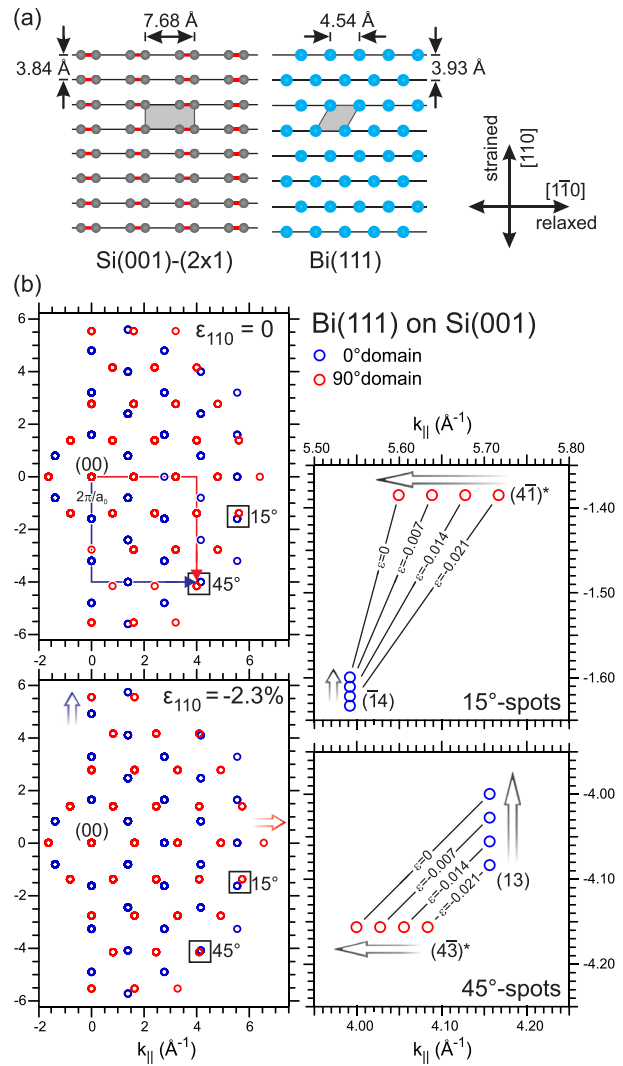


**FIG. 1.** (a) Lattice accommodation of Bi(111) on Si(001). Along  $[1\bar{1}0]$ , 11 Bi atoms fit on 13 Si atoms. Along  $[110]$ , the Bi row distance of 3.93 Å can be accommodated to the Si row distance of 3.84 Å upon compression by 2.3%. (b) Schematic LEED patterns for two hexagonal Bi(111) surfaces which are rotated by 90° with respect to each other. Upper left panel: relaxed film. Lower left panel: by 2.3% anisotropically strained film. Two pairs of higher order spots are indicated (15° and 45°) which are very close. Right panels show the motion of these pairs of spots upon relaxation of the film.

Bi(111) film towards the bulk value with  $\epsilon_{110} = 0$ . For the 15° spots, the relative distance does not change much. However, the relative orientation of the two spots varies strongly. From the determination of the relative distance of such pairs of spots, the anisotropic strain state of the film could be easily determined. This magnifying glass works better the closer the pairs of spots are and the higher the order of the used integer order spots are. In this letter, we concentrate only on the evaluation of the 45° spots because the relative motion of the 45° spots is symmetric and larger than that for the 15° spots.

The experiments have been performed under ultra-high vacuum conditions at a base pressure of  $2 \times 10^{-10}$  mbar using high-resolution SPA-LEED.<sup>12–14</sup> Si(001) samples (Boron doped, 8–12- $\Omega$ cm, miscut less than 0.2°) have been prepared after degassing at 600 °C by a short flash annealing cycle up to 1350 °C. The presence of a clear  $c(4 \times 2)$  reconstruction at 150 K serves as proof for a clean surface. Sample cooling was carried out using a liquid nitrogen cryostat attached to the sample holder. High purity Bi (Mateck GmbH, purity 99.9999%) was evaporated from a directly heated ceramic crucible mounted in a water-cooled copper shroud. The deposition rate of the Bi film was monitored using a quartz microbalance mounted on the evaporator. The coverage was calibrated by the observation of bilayer intensity oscillations of the (00)-spot during Bi deposition.<sup>17</sup> As an initial step for every growth experiment, a thin high quality Bi(111) base film was prepared on the Si(001) substrate following a recipe described by Jnawali *et al.*,<sup>15</sup> which results in extremely smooth Bi(111) surfaces with large terraces.<sup>16</sup> This kinetic pathway is necessary to avoid islanding of Bi. Thicker films were grown by subsequent deposition at 450 K up to the desired thickness. A deposition rate of 1.0 bilayer/min ( $1 \text{ BL}_{\text{Bi}} = 1.14 \times 10^{15} \text{ cm}^{-2}$ ) was maintained during each deposition process. Due to the pronounced Debye-Waller effect on Bi surfaces, all LEED patterns have been taken at 80 K. The slight distortion of SPA-LEED patterns occurring at higher diffraction angles was compensated by a remapping process<sup>18</sup> which was calibrated using the well-defined LEED pattern of the Si(001) substrate.

Figure 2(a) shows the diffraction pattern of a 26 nm thick Bi(111) film which is almost relaxed to the Bi bulk lattice parameter.<sup>16</sup> The superposition of the two diffraction patterns rotated by 90° is clearly seen. The pair of spots, which was used for the evaluation, is marked by 45°. This pair of spots is plotted in Fig. 2(b) with higher magnification for 4.3 nm, 6.6 nm, and 26 nm thick Bi films. The expected spot positions for a 2.3% compressively strained commensurable film are marked by the black dots with a separation of 5.6% of  $2\pi/a_0$ . The white crosses mark the expected spot positions for a fully relaxed Bi film with a separation of 13.9% of  $2\pi/a_0$ .

The three snapshots show a clear increase in spot separation and a symmetric shift of the spot position for the 45° spots from the strained (4.3 nm) to relaxed (26 nm) state. At a coverage of 6.6 nm, the spots are elongated and split into a series of satellites, reflecting the presence of a dislocation array confined to the interface accommodating the 2.3% lattice mismatch.<sup>15</sup> The Burgers vector  $\mathbf{b}$  of the misfit dislocation is equal to the surface lattice spacing of the Si(001) substrate, i.e.,  $\mathbf{b} = \frac{1}{2}[110]$  parallel to the heterointerface and with an edge component of  $b_{\parallel, \text{edge}} = a_{\text{Si}(001)} = 3.84 \text{ \AA}$ .<sup>19</sup> The periodic arrangements of these dislocations elastically distort the Bi film and lead to a weak undulation of the Bi surface which acts as a phase grating with a period of  $\sim 20$  nm for the electrons.<sup>20–22</sup> In the bottom right panel of Fig. 2, the motion of the spots is shown by open circles of increasing size to indicate increasing film thickness. As expected, the spots move along straight lines towards the positions of the bulk Bi.

For a precise analysis of the spot position, the center of mass of the spot's intensity was determined. The maximum of the 45°-spots from Fig. 2(b) would only give the most likely

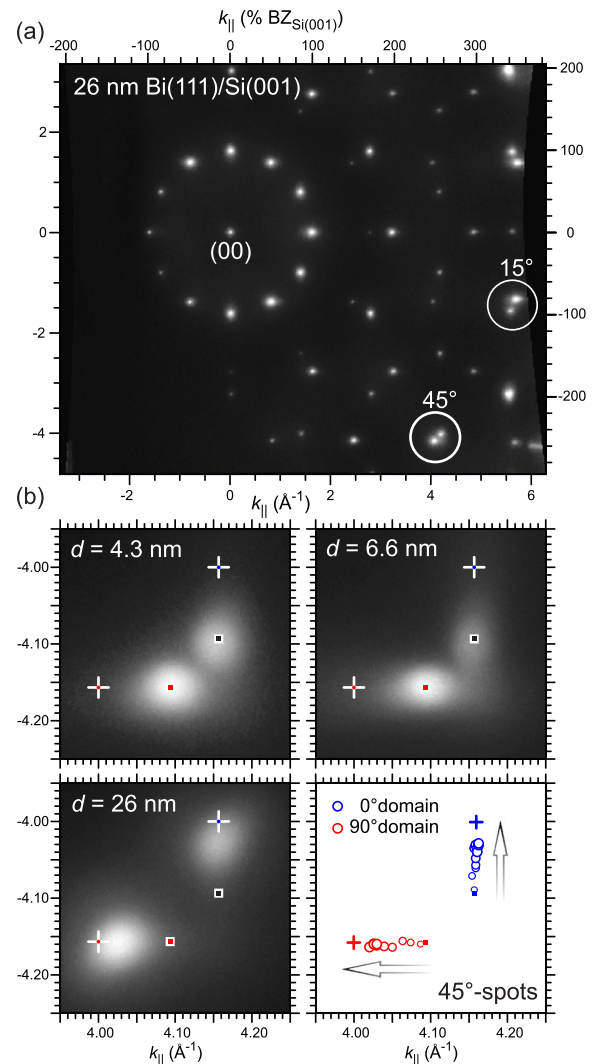


**FIG. 2.** (a) SPA-LEED pattern of a 26 nm Bi(111) film on Si(001). The two by 90° rotated hexagonal patterns are present. The pairs of spots of 4th order which are very close are indicated by 15° and 45°. (b) Motion of the spots with increasing thickness for 4.3 nm (strained film), 6.6 nm (relaxation by the misfit dislocation array), and 26 nm (almost relaxed film). In the lower right panel, the motion of the spot position with the increasing film thickness is plotted. Crosses indicate the spot positions for complete relaxation, i.e., bulk lattice parameter. Squares indicate the spot positions for a fully strained film, i.e., coherent to the substrate.

lattice distance. The center of mass, however, gives the average lattice parameter and naturally accounts for spot broadening due to roughness, dislocations, or defects in the film. These values for the lattice parameter are plotted in Fig. 3(a) as a function of film thickness for Bi films with initial thicknesses of 4.3 nm and 6.6 nm. Measurements were performed at 80 K after a successive increase in the film thickness through deposition of small amounts of additional Bi at 450 K. Both films show the same relaxation behavior. We observe an increase in the lattice parameter of the Bi(111) film from 3.84 Å at a thickness of 4.3 nm to 3.91 Å at a thickness of 26 nm.

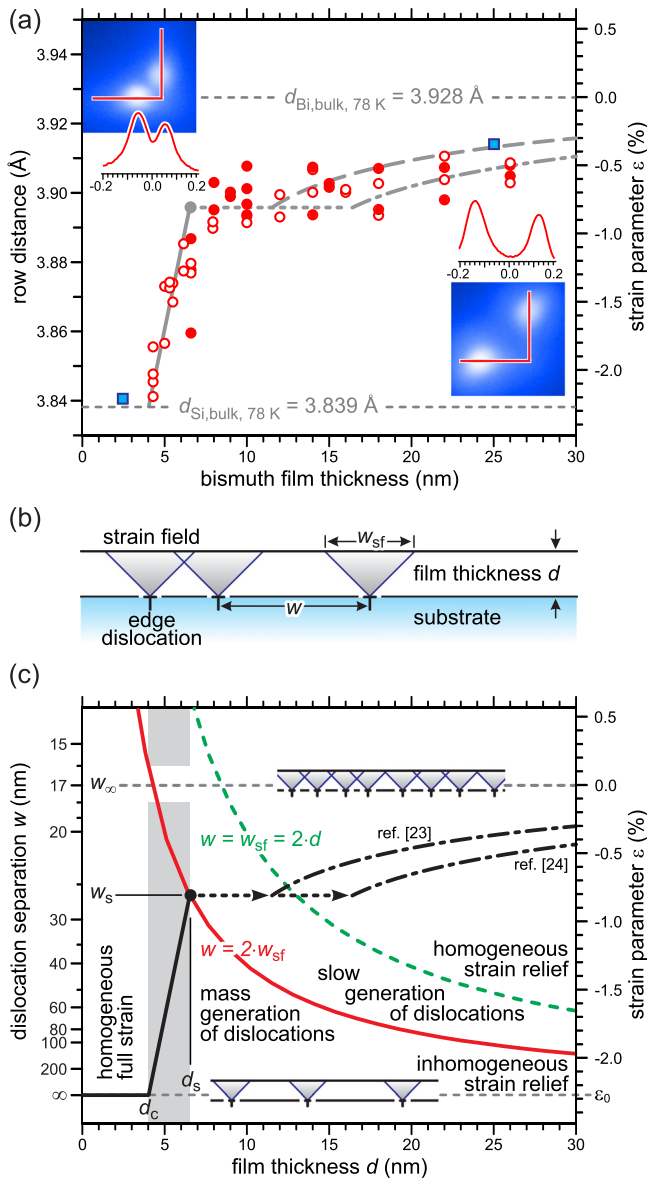


**FIG. 3.** (a) Strain state and relaxation of Bi(111) films on Si(001) as a function of thickness. Open red circles and red dots are the data from different initial film thicknesses of 4.3 nm and 6.6 nm. The insets show 45° LEED spots and spot profiles for film thicknesses of 4.3 nm and 26 nm. Profiles were taken along an angulated path as indicated in the LEED pattern. Filled blue squares depict the films grown directly to the desired thickness. (b) Sketch of strain fields emerging at the interfacial misfit dislocations. The width  $w_{\text{sf}}$  of the strain fields is twice the film thickness  $d$ . Interaction of dislocations sets in as soon as  $w < w_{\text{sf}}$ , i.e., when strain fields start to overlap each other. (c) Phase diagram of the strain relief mechanism by interfacial misfit dislocations for heterofilms. The width of the strain field  $w_{\text{sf}}$  (dashed green line) is proportional to twice the thickness  $d$  of the film. The solid red line indicates the condition  $w < 2w_{\text{sf}}$  when the massive generation of dislocations stops because their density becomes too high. The solid black dot indicates the transition at  $d = 6.5 \text{ nm}$  from massive generation to slow generation of dislocations. The dashed dotted lines describe the regime of slow generation of dislocations as described in Refs. 23 and 24.

The measured value for the critical film thickness  $d_c = 4 \text{ nm}$  for the generation of the first misfit dislocations agrees with the expected values of 4.5 nm and 7 nm from theories of van der Merwe<sup>23</sup> and Matthews,<sup>24</sup> respectively. This agreement surprises as these models refer to thermodynamic equilibrium, and the experimental critical thickness usually exceeds the theoretical values owing to low substrate temperatures. In our case, the Bi films were grown at a seemingly very low substrate temperature of 150 K. However, keeping in mind the low melting temperature of 271°C and the still high mobility of Bi atoms even at  $T = 80 \text{ K}$  (Ref. 17) the activation energy for bond breaking and nucleation of dislocations is also reduced.

The sudden and strong onset of strain relief, however, is not explained within these theories, which describe systems with a homogenous strain state.<sup>23–26</sup> With these theories, a smooth onset of strain relief and long-lasting continuous generation of misfit dislocations is expected. In contrast to this expectation, we observe a massive generation of misfit dislocations between film thicknesses of 4 nm and 7 nm, already resulting in a strain relief of 65%.

We explain this behavior by the local confinement of the strain relief associated with a misfit dislocation. Each edge-type dislocation is surrounded by an elastic strain field  $\mathbf{u}(x, z)$  which causes lateral and vertical displacements of the Bi (and Si) lattice sites normal to the dislocation line. These strain fields usually exhibit a Lorentzian shape  $\mathbf{u}(x, z) \propto d^2/(x^2 + d^2)$  and expand laterally proportional to the increasing film thickness  $d$ .<sup>27,28</sup> The full width  $w_{\text{sf}}$  at half maximum of the amplitude of the strain field  $\mathbf{u}(x, z)$  is twice the film thickness  $d$ . Thus, the strain relief induced by a single dislocation is confined to a volume with a triangular cross-section of width  $w_{\text{sf}} = 2d$  above the dislocation line. Consequently, the strain state is highly inhomogeneous across a film: between dislocations of a distance  $w > 2d$ , the film is still fully strained. With further increasing thickness, these still strained areas of the film will be relaxed almost instantaneously by the generation of further dislocations. This massive generation of dislocations stops as soon as the width of the still strained areas becomes smaller than  $w_{\text{sf}}$ , i.e., the dislocations exhibit an average separation of  $w < 2w_{\text{sf}} = 4d$ . This situation is sketched in Fig. 3(c) for a heterofilm with a lattice mismatch of 2.3% and a critical thickness of  $d_c = 4 \text{ nm}$ . The inverse separation of dislocations, i.e., their density, is plotted as a function of film thickness  $d$ . The solid red hyperbola reflects the above-mentioned condition  $w = 2w_{\text{sf}} = 4d$ . In the regime below the hyperbola, the film exhibits a spatially inhomogeneous strain state and existing dislocations are separated by more than 4 times the film thickness  $d$ . Then, massive generation of dislocations sets in at the critical thickness  $d_c$  and stops when the separation between the strain fields is smaller than  $w_{\text{sf}}$ . In our case, this transition between massive generation and slow generation is expected as soon as the distance between dislocations  $w$  (solid black line) crosses the hyperbola at  $w_s = 26 \text{ nm}$  and  $d = 6.5 \text{ nm}$ . At this point, nearly 2/3 of the strain of the Bi film (65% of total strain) is already relieved.

The dashed green hyperbola indicates the condition  $w = w_{\text{sf}} = 2d$  when the strain fields start to overlap and the dislocations interact repulsively. Thus, in the regime above the

dashed hyperbola, the film exhibits a homogenous strain state. The continuous and slow generation of dislocations is then governed by existing theory,<sup>23,24</sup> which is described by the two dashed dotted lines, and sets in for  $d = 12$  nm. For thicker films, i.e.,  $d \rightarrow \infty$ , we expect an asymptotic behavior of the strain relief towards the bulk lattice parameter and an average distance of  $w_\infty = 17$  nm between the dislocations.

In summary, we observed a lattice mismatch induced strain and its relaxation through interfacial misfit dislocations during heteroepitaxial growth of Bi(111) on Si(001). The strain state of the Bi film is precisely determined by analyzing relative changes of spot positions in SPA-LEED up to 4th order spots. The thickness dependent strain relief kinetics follow a phase diagram with an initial steep onset at a critical thickness of 4 nm followed by a slow and continuous strain relief beyond 7 nm. The unusual steep onset is explained by inhomogeneous strain relief through massive generation of locally confined dislocations, which turn into homogeneous strain relief as the heterofilm grows and the strain fields interact with each other. These findings not only are limited to Bi on the Si system but also are of general importance for the understanding of strain relaxation in heteroepitaxial film growth.

Financial support of the Deutsche Forschungsgemeinschaft (DFG, German Research Foundation) through Collaborative Research Center SFB1242 “Non-equilibrium dynamics of condensed matter in the time domain” (Project No. 278162697) is gratefully acknowledged.

## REFERENCES

- <sup>1</sup>F. Capasso, “Band-gap engineering: From physics and materials to new semiconductor devices,” *Science* **235**, 172 (1987).
- <sup>2</sup>Y. Suna, S. E. Thompson, and T. Nishida, “Physics of strain effects in semiconductors and metal-oxide-semiconductor field-effect transistors,” *J. Appl. Phys.* **101**, 104503 (2007).
- <sup>3</sup>C. Zh. Ning, L. Dou, and P. Yang, “Bandgap engineering in semiconductor alloy nanomaterials with widely tunable compositions,” *Nat. Rev. Mater.* **2**, 17070 (2017).
- <sup>4</sup>S. Chattopadhyay, L. D. Driscoll, K. S. K. Kwa, S. H. Olsen, and A. G. O’Neill, “Strained Si MOSFETs on relaxed SiGe platforms: Performance and challenges,” *Solid-State Electron.* **48**, 1407 (2004).
- <sup>5</sup>S. W. Bedell, A. Khakifirooz, and D. K. Sadana, “Strain scaling for CMOS,” *MRS Bull.* **39**, 131 (2014).
- <sup>6</sup>S. Pimputkar, J. S. Speck, S. P. DenBaars, and S. Nakamura, “Prospects for LED lighting,” *Nat. Photonics* **3**, 180 (2009).
- <sup>7</sup>A. I. Alhassan, N. G. Young, R. M. Farrell, C. Pynn, F. Wu, A. Y. Alyamani, S. Nakamura, S. P. DenBaars, and J. S. Speck, “Development of high performance green c-plane III-nitride light-emitting diodes,” *Opt. Express* **26**, 5591 (2018).
- <sup>8</sup>P. P. Li, Y. B. Zhao, H. J. Li, J. M. Che, Z.-H. Zhang, Z. C. Li, Y. Y. Zhang, L. C. Wang, M. Liang, X. Y. Yi, and G. H. Wang, “Very high external quantum efficiency and wall-plug efficiency 527 nm InGaN green LEDs by MOCVD,” *Opt. Express* **26**, 33108 (2018).
- <sup>9</sup>Y. Zhao, H. Fu, G. T. Wang, and S. Nakamura, “Toward ultimate efficiency: Progress and prospects on planar and 3D nanostructured nonpolar and semipolar InGaN light-emitting diodes,” *Adv. Opt. Photonics* **10**, 246 (2018).
- <sup>10</sup>M. Horn-von Hoegen, M. Pook, A. A. Falou, B. H. Müller, and M. Henzler, “The interplay of surface morphology and strain relief in surfactant mediated growth of Ge on Si(111),” *Surf. Sci.* **284**, 53 (1993).
- <sup>11</sup>A. I. Nikiforov, V. A. Cherepanov, O. P. Pchelyakov, A. V. Dvurechenskii, and A. I. Yakimov, “In situ RHEED control of selforganized Ge quantum dots,” *Thin Solid Films* **380**, 158 (2000).
- <sup>12</sup>M. Horn-von Hoegen, “Growth of semiconductor layers studied by spot profile analysing low energy electron diffraction – Part I,” *Z. Kristallogr.* **214**, 591 (1999).
- <sup>13</sup>M. Horn-von Hoegen, “Growth of semiconductor layers studied by spot profile analysing low energy electron diffraction – Part II,” *Z. Kristallogr.* **214**, 684 (1999).
- <sup>14</sup>U. Scheithauer, G. Meyer, and M. Henzler, “A new LEED instrument for quantitative spot profile analysis,” *Surf. Sci.* **178**, 441 (1986).
- <sup>15</sup>G. Jnawali, H. Hattab, B. Krenzer, and M. Horn-von Hoegen, “Lattice accommodation of epitaxial Bi(111) films on Si(001) studied with SPA-LEED and AFM,” *Phys. Rev. B* **74**, 195340 (2006).
- <sup>16</sup>H. Hattab, E. Zubkov, A. Bernhart, G. Jnawali, C. Bobisch, B. Krenzer, M. Acet, R. Möller, and M. Horn-von Hoegen, “Epitaxial growth of thin, low defect Bi films on Si(001): strain state, surface morphology and defects,” *Thin Solid Films* **516**, 8227 (2008).
- <sup>17</sup>G. Jnawali, H. Hattab, C. A. Bobisch, A. Bernhart, E. Zubkov, R. Möller, and M. Horn-von Hoegen, “Homoepitaxial growth of Bi(111),” *Phys. Rev. B* **78**, 035321 (2008).
- <sup>18</sup>See <http://www.wavemetrics.com> for details of the remapping procedure.
- <sup>19</sup>G. Jnawali, H. Hattab, F.-J. Meyer zu Heringdorf, B. Krenzer, and M. Horn-von Hoegen, “Lattice-matching periodic array of misfit dislocations: Heteroepitaxy of Bi(111) on Si(001),” *Phys. Rev. B* **76**, 035337 (2007).
- <sup>20</sup>U. Gradmann and G. Waller, “Periodic lattice distortions in epitaxial films of Fe(110) on W(110),” *Surf. Sci.* **116**, 539 (1982).
- <sup>21</sup>M. Horn-von Hoegen, A. Al-Falou, H. Pietsch, B. Müller, and M. Henzler, “Formation of the interfacial dislocation network in surfactant-mediated growth of Ge on Si(111) by SPALEED,” *Surf. Sci.* **298**, 29 (1993).
- <sup>22</sup>M. Horn-von Hoegen and M. Henzler, “Lattice matching periodic interfacial dislocation network in surfactant-mediated growth of Ge on Si(111),” *Phys. Status Solidi (a)* **146**, 337 (1994).
- <sup>23</sup>J. H. Van Der Merwe, “Crystal interfaces. Part II. Finite overgrowths,” *J. Appl. Phys.* **34**, 123 (1963).
- <sup>24</sup>J. W. Matthews, “Defects associated with the accommodation of misfit between crystals,” *J. Vac. Sci. Technol.* **12**, 126 (1975).
- <sup>25</sup>R. People and J. C. Bean, “Calculation of critical layer thickness versus lattice mismatch for  $\text{Ge}_x\text{Si}_{1-x}/\text{Si}$  strained-layer heterostructures,” *Appl. Phys. Lett.* **47**, 322 (1985); **49**, 229 (1986).
- <sup>26</sup>S. M. Hu, “Misfit dislocations and critical thickness of heteroepitaxy,” *J. Appl. Phys.* **69**, 7901 (1991).
- <sup>27</sup>F. R. N. Nabarro, *Theory of Crystal Dislocations* (Dover, New York, 1987).
- <sup>28</sup>G. Jnawali, H. Hattab, C. A. Bobisch, A. Bernhart, E. Zubkov, R. Möller, and M. Horn-von Hoegen, “Nanoscale dislocation patterning in Bi(111)/Si(001) heteroepitaxy,” *Surf. Sci.* **603**, 2057 (2009).